Cardiovascular Research (2008) **79**, 416–426
doi:10.1093/cvr/cvn100

Enhancement of ventricular gap-junction coupling by rotigaptide

Xianming Lin[1], Christian Zemlin[1], James K. Hennan[2], Jørgen S. Petersen[3], and Richard D. Veenstra[1]*

[1]*Department of Pharmacology, SUNY Upstate Medical University, 750 East Adams Street, Syracuse, NY 13210, USA;* [2]*Cardiovascular and Metabolic Disease, Wyeth Research, Collegeville, PA 19426, USA; and* [3]*Zealand Pharma A/S, Department of Pharmacology, Glostrup, Denmark*

Received 4 January 2008; revised 4 April 2008; accepted 10 April 2008; online publish-ahead-of-print 22 April 2008

Time for primary review: 23 days

KEYWORDS
Antiarrhythmic agents;
Cell communication;
Connexins;
Gap junctions;
Rotigaptide

Aims Rotigaptide is proposed to exert its anti-arrhythmic effects by improving myocardial gap-junction communication. To directly investigate the mechanisms of rotigaptide action, we treated cultured neonatal murine ventricular cardiomyocytes with clinical pharmacological doses of rotigaptide and directly determined its effects on gap-junctional currents.

Methods and results Neonatal murine ventricular cardiomyocytes were enzymatically isolated and cultured for 1–4 days. Primary culture cell pairs were subjected to dual whole cell patch-clamp procedures to directly measure gap-junctional currents (I_j) and voltage (V_j). Rotigaptide (0–350 nM) was applied overnight or acutely perfused into 35 mm culture dishes. Rotigaptide (35–100 nM) acutely and chronically increased the resting gap-junction conductance (g_j), and normalized steady-state minimum g_j (G_{min}) by 5–20%. Higher concentrations produced a diminishing response, which mimics the observed therapeutic efficacy of the drug. The inactivation kinetics was similarly slowed in a therapeutic concentration-dependent manner without affecting the V_j dependence of inactivation or recovery. The effects of 0–100 nM rotigaptide on ventricular g_j during cardiac action potential propagation were accurately modelled by computer simulations which demonstrate that clinically effective concentrations of rotigaptide can partially reverse conduction slowing due to decreases in g_j and inactivation.

Conclusion These results demonstrate that therapeutic concentrations of rotigaptide increase the resting gap-junction conductance and reduce the magnitude and kinetics of steady-state inactivation in a concentration-dependent manner. Rotigaptide may be effective in treating re-entrant forms of cardiac arrhythmias by improving conduction and preventing the formation of re-entrant circuits in partially uncoupled myocardium.

1. Introduction

Uniform coupling of myocardial cells by gap junctions is essential to the rapid, synchronous electrical activation and initiation of contraction vital to cardiac function. The heterogeneous loss of ventricular Cx43 expression not only compromises the electrophysiological activation and refractory properties of the myocardium to produce a highly arrhythmogenic substrate, but also the contractile function of the heart.[1–3] Rotigaptide is a novel antiarrhythmic peptide that exerts its effects on re-entrant forms of ventricular tachycardias by improving electrical cell–cell coupling.[4–6] Rotigaptide, a D-isomer analogue of the antiarrhythmic hexapeptide AAP10, increases Cx43-mediated gap-junction communication, reduces ischaemia-induced infarct size and conduction slowing, and prevents spontaneous ventricular arrhythmias in various cell and animal models.[7–10] Rotigaptide has been advanced into clinical development and the safety evaluation from phase I studies in healthy volunteers looks very promising.[11]

To further elucidate the possible mechanisms of action of rotigaptide on cardiac gap junctions, we investigated the effects of rotigaptide treatment on the gating of ventricular gap junctions using the dual whole cell action potential voltage clamp method.[12] Previously, the kinetic modelling of ventricular gap-junction gating over the duration of the ventricular action potential at various frequencies revealed that significant inactivation can develop during the first 25 ms of an action potential that can contribute to further conduction slowing and eventual conduction block.[13] It was further demonstrated that ventricular gap junctions recovered from the inactivation induced by the action potential-derived transjunctional voltage (V_j) gradients beginning with phase 3 repolarization. Gap-junction conductance (G_j) actually increases above initial peak values during the final recovery phase at a time when the ventricular myocardium is most susceptible to re-entrant or triggered

* Corresponding author. Tel: +1 315 464 5145; fax: +1 315 464 8014.
E-mail address: veenstrr@upstate.edu

activity that gives rise to spontaneous ectopic activity.[14,15] In the present study, we demonstrate that rotigaptide has a concentration-dependent effect on the magnitude and kinetics of ventricular gap-junction conductance and inactivation. These effects were observed at clinically relevant concentrations of rotigaptide and declined with increasing doses above 100 nM. Finally, we developed model parameters for the action of rotigaptide on the inactivation of ventricular gap junctions. Computer simulations of action potential propagation demonstrate that, by increasing gap-junction conductance and slowing inactivation, rotigaptide can counteract conduction slowing in partially uncoupled myocardium during discontinuous propagation.

2. Methods

All experiments were performed on enzymatically dissociated neonatal C57Bl/6 murine ventricular myocytes cultured for 48–72 h according to published procedures.[12] The investigation conforms with the *Guide for the Care and Use of Laboratory Animals* published by the US National Institutes of Health (NIH Publication No. 85-23, revised 1996). A 100 μM rotigaptide stock solution was prepared fresh weekly and stored at 4°C. This stock solution was added to the M199/10% foetal bovine serum myocyte culture media and the cells incubated overnight at 37°C in a humidified 5% CO_2 atmosphere after >24 h in culture. Rotigaptide was also present during all patch-clamp experiments. Dual whole cell patch-clamp experiments were performed at room temperature (20–22°C) using a static or perfused (1 mL/min) bath volume of 3 mL HEPES-buffered, balanced salt saline (pH 7.4) according to established procedures.[16]

A series of three distinct voltage clamp protocols were performed on rotigaptide-treated ventricular myocytes. The 1/s ventricular action potential waveform and 200 ms/mV transjunctional voltage (V_j) ramps were performed on ventricular myocytes treated with 0, 20, 35, 50, 100, 200, or 350 nM rotigaptide.[12] A minimum of six different cell pair gap-junction current (I_j) recordings were obtained for each test concentration and the results were averaged for curve fitting analysis of the action potential kinetic and steady-state V_j-dependent gating parameters. Each experimental I_j result represented the ensemble average of 100 action potential waveforms or five complete $\pm V_j$ ramp protocols. The actual applied V_j was determined for these ensemble averaged I_j traces using Eq. (1):

$$V_j = [V_1 - (R_{el1} \cdot I_1) - V_2 + (R_{el2} \cdot I_2)]. \quad (1)$$

The junctional conductance (g_j) was calculated as $g_j = -\Delta I_2 / V_j$.[16] These procedures account for the series resistance voltage drop ($V_{series} = I_{cell} \cdot R_{el}$) across the whole cell patch electrode resistance (R_{el}) as a function of the whole cell current ($I_{1\ or\ 2}$) for each cell relative to the command potential ($V_{1\ or\ 2}$). Pooled data for each experimental group and V_j protocol were normalized either to the junctional conductance (G_j) value at the peak of action potential or the linear slope conductance of the I_j–V_j relationship at low V_j values.[12]

Analysis of the first-order inactivation kinetics required ensemble averaged signals from 5 to 10 square V_j pulses ranging from +70 to +140 mV. The ensemble averaged I_j traces were fit with biexponential decaying functions to obtain the decay time constants (τ_{decay}) from which the fast and slow closing (on)-rates for the V_j-dependent inactivation processes were calculated. The inactivation on-rates (k_{on}) were calculated using the expression [Eq. (2)]:

$$k_{on} = (1 - P_o)/\tau_{decay}. \quad (2)$$

The open probability, P_o, was calculated as the remaining fraction of I_j at the end of the V_j pulse (=steady-state I_j/peak I_j). The calculated fast and slow on-rates were plotted as a function of V_j and fit with a single exponential function of the form [Eq. (3)]:

$$k_{on} = A \cdot \exp(V_j / V_{k,on}) + C, \quad (3)$$

where A is the rate amplitude, $V_{k,on}$ the predicted voltage constant for the inactivation rate, and C the minimum rate amplitude. This inactivation kinetic analysis was performed for only control and low or optimal rotigaptide concentrations. Examples of the voltage clamp protocols used in the kinetic and steady-state g_j analyses are provided in the Supplementary material, online.

3. Results

3.1 Voltage-dependent gating of ventricular gap junctions

Continuous exposure to a constant concentration of rotigaptide produced dose-dependent changes in the gating of ventricular gap junctions during pacing with the 1 s basic cycle length (BCL) Luo–Rudy model ventricular action potential waveform.[17] The ensemble-averaged I_j responses to the V_j gradient resulting from a train of 100 action potentials applied to cell 1 with cell 2 clamped to the resting potential (−89.8 mV) are shown for control and 100 nM rotigaptide conditions (*Figure 1A* and *B*). The action potential derived V_j gradients were essentially identical for both experiments and the peak g_j was also similar between these two representative experiments. The time course of the inactivation is different between the control and the rotigaptide treatment groups, indicative of a pharmacological effect on the gating of cardiac g_j. After normalization to the peak g_j from each experiment ($G_{max} = 1$), the averaged G_j (=normalized g_j) data for each test concentration of rotigaptide are displayed in *Figure 1C* and *D*. The mean g_j values (±SEM) were 2.86 ± 0.72 nS, 3.37 ± 1.04 nS, 2.84 ± 0.85 nS, 2.64 ± 0.39 nS, 3.44 ± 0.81 nS, 1.56 ± 0.46 nS, and 1.56 ± 0.59 nS for the 0, 20, 35, 50, 100, 200, and 350 nM rotigaptide experiments. The slowing of inactivation and the reduction in plateau inactivation during the action potential increased with increasing [rotigaptide] between 20 and 100 nM and declined nearly back to control values as [rotigaptide] was increased further to 350 nM. This biphasic dose–response curve indicates an optimal effective range of [rotigaptide] on the inhibition of g_j inactivation of ≤100 nM under standard cell culture conditions. This observation is in agreement with previous findings of a bell-shaped dose–response curve for the effect of rotigaptide on conduction velocity in atrial strips experiencing metabolic stress.[8]

In a separate set of experiments, the rate dependence of 100 nM rotigaptide was examined using the 250 and 500 ms BCL action potentials (*Figure 1E* and *F*). Again, there were no significant differences in the mean g_j values between control and 100 nM rotigaptide groups. The average g_j was 2.83 ± 1.00 ($n = 6$) and 3.88 ± 1.54 nS ($n = 6$) for the control and 3.44 ± 1.21 ($n = 6$) and 3.49 ± 1.46 nS ($n = 7$) for the 100 nM rotigaptide experiments at BCL = 250 and 500 ms, respectively. These data demonstrate that rotigaptide had a similar effect on the 2 or 4 Hz action potentials as on the standard 1 Hz ventricular action potential waveform. Slowing of inactivation and an increase in G_{min} is evident at all stimulation frequencies. Slower frequencies were not examined since no further increase in inactivation was previously observed with longer action potential

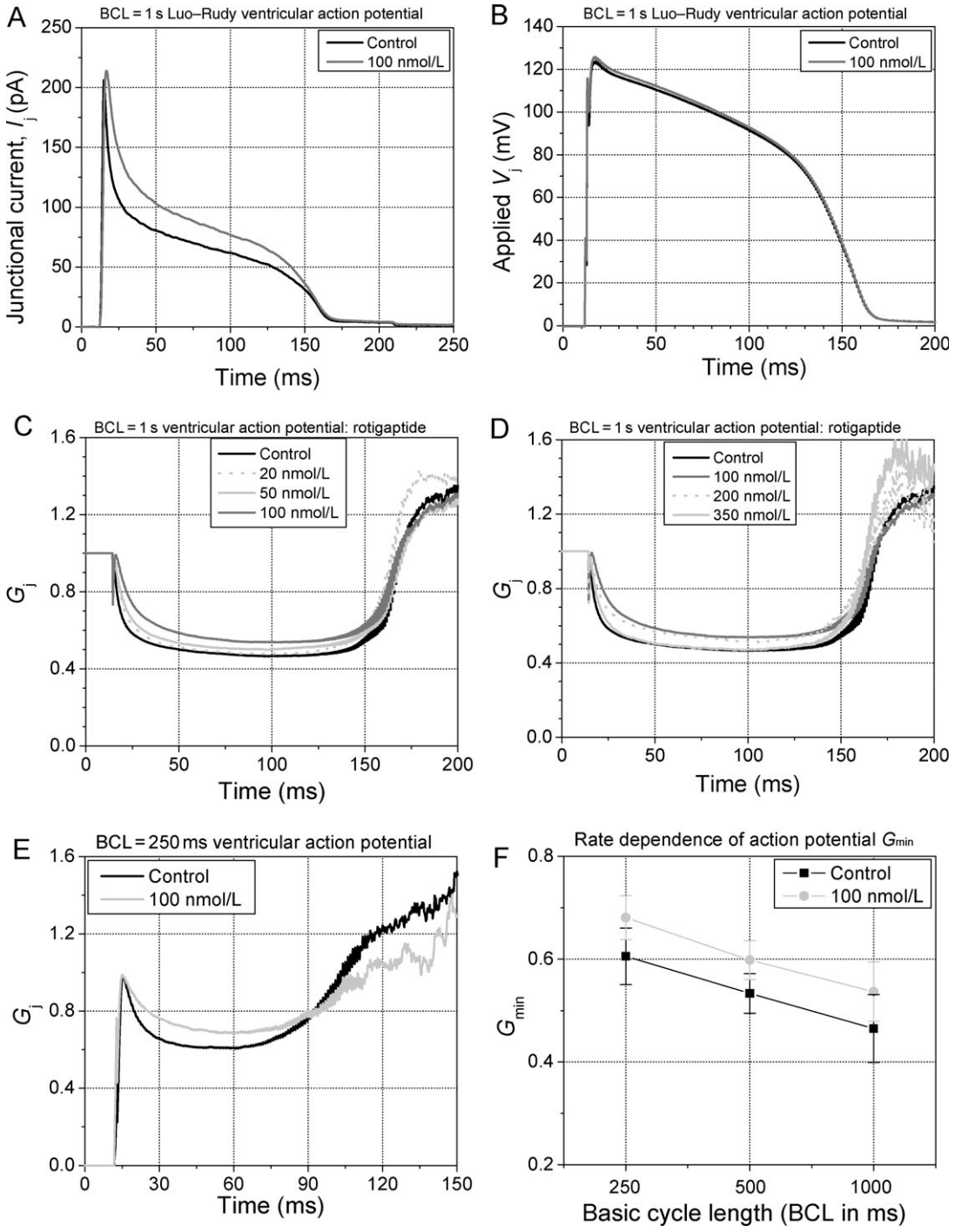

Figure 1 Gating of ventricular gap junctions during an action potential. (*A*) Ensemble averaged I_j traces from two separate experiments of similar g_j, one untreated (black) and one treated ventricular myocte cell pair with 100 nM rotigaptide (grey). I_j was increased in the rotigaptide experiment relative to the control recording. (*B*) The applied V_j gradients were virtually identical for both experiments. (*C*) Continuous rotigaptide treatment consistently reduced the rate and magnitude of inactivation in a concentration-dependent manner from 0 to 100 nM. (*D*) Above 100 nM, the rotigaptide effect was diminished, returning almost to control values at 350 nM. $N = 6$ experiments/concentration. (*E*) Reduction of G_j inactivation by 100 nM rotigaptide during rapid pacing using the 250 mS basic cycle length (BCL) ventricular action potential. (*F*) 100 nM rotigaptide decreased the magnitude of G_j inactivation at all stimulation frequencies >1 Hz.

durations (APDs) and BCLs.[12] Constant pacing at BCL = 1000 ms with the short, triangular neonatal murine action potential waveform also demonstrated an enhancement of I_j with 100 nM rotigaptide treatment (see Supplementary material online, *Figure S4*).[18]

The effect of rotigaptide on the steady-state G_j–V_j relationship was also examined using a 200 ms/mV continuous V_j ramp of ± 120 mV. This provides a measure of the magnitude of the time-independent G_j inactivation. A Boltzmann equation fit of the experimental curves provides a measure of the half-inactivation voltage ($V_{1/2}$), the V_j-sensitivity (valence, z), and the V_j-insensitive portion of the total G_j (G_{min}, *Figure 2A*; see also Supplementary material, online). G_{max} was taken as the linear slope conductance during the rising phase of V_j for each polarity. Reversing the direction of the V_j ramp from its maximum value

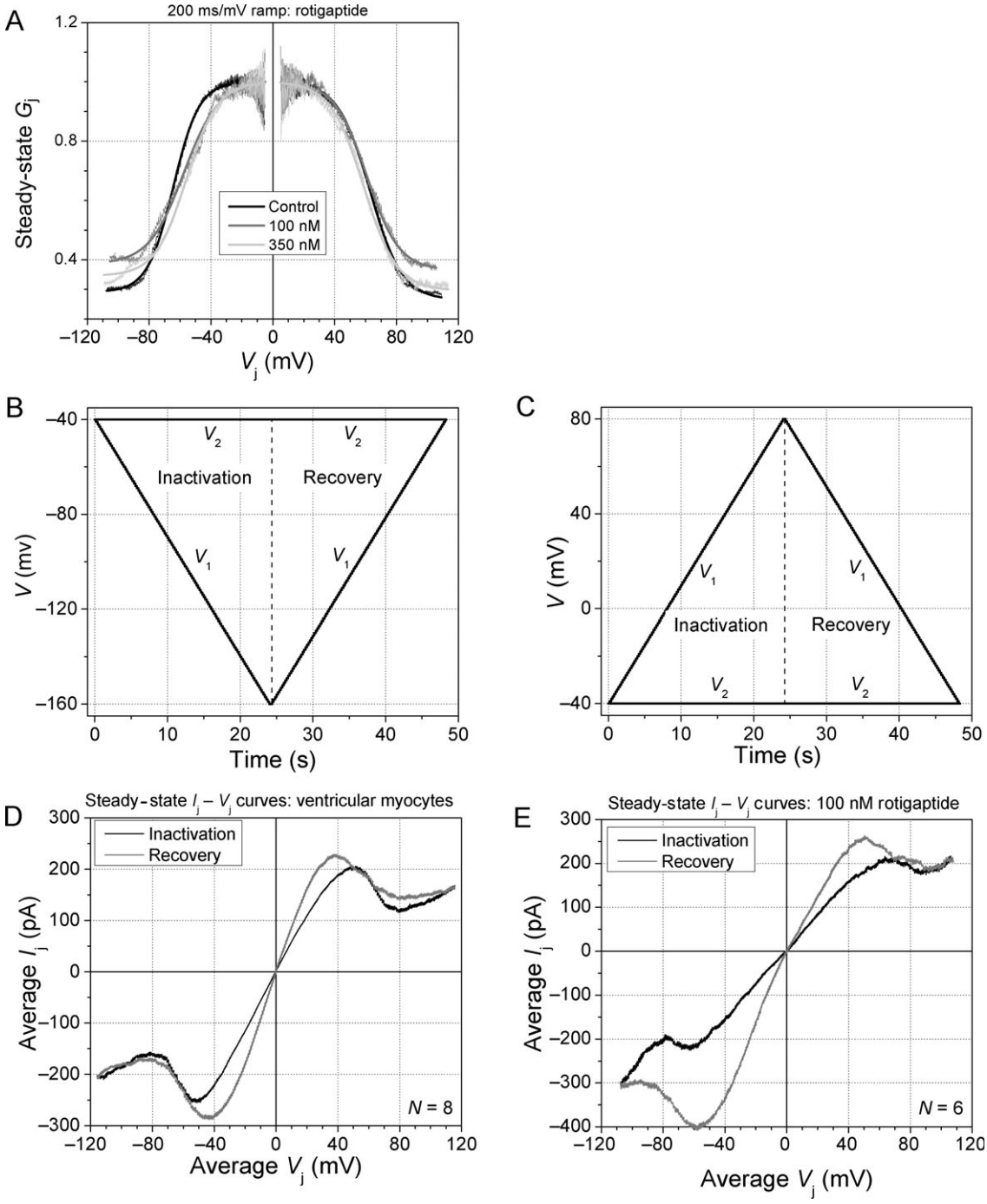

Figure 2 Effects of rotigaptide on steady-state ventricular G_j inactivation and recovery. (*A*) 100 nM rotigaptide produced the maximal effect of increasing the G_{min} of the steady-state G_j–V_j curves whereas this effect was almost completely reversed by a 350 nM dose. (*B* and *C*) Command voltage protocols for the negative (*B*) and positive (*C*) V_j inactivation and recovery ramps. (*D*) The normalized I_j (=G_j·V_j)–V_j relationship for the rising phase (black) and the falling phase (grey) of the $\pm$120 mV V_j ramp reveals the increased slope conductance, called facilitation, during the recovery from inactivation in ventricular myocytes. (*E*) The same V_j protocol applied to 100 nM rotigaptide-treated ventricular myocytes demonstrates the reduction of inactivation during the rising phase of the ramp, but a negligible effect on the return (recovery) phase of the V_j ramp.

provides a similar description of the steady-state G_j recovery and, most notably, the facilitation of G_j originally observed in cardiomyocyte gap junctions composed predominantly of Cx43 (*Figure 2B–E*).[12] The I_j–V_j curves displayed in *Figure 2D* and *E* again demonstrate a reduction in the magnitude of ventricular gap-junction inactivation by rotigaptide with no apparent effect on the increased slope G_j during the return phase (i.e. facilitation = $G_{max,\ rec}$) of the slow V_j ramp.

The concentration-dependent effects of rotigaptide on the V_j-insensitive G_{min} of the inactivation and the $G_{max,\ rec}$ of the steady-state G_j–V_j curves are summarized in *Figure 3*. The 10% increase in G_{min} was statistically different from control values for the maximal effective dose of 100 nM rotigaptide ($P < 0.05$, student's *t*-test) and was similar for the action potential and V_j ramp voltage clamp protocols (*Figure 3A*). Since all g_j values were normalized to the initial slope g_j for each experiment (i.e. $G_{max} = 1$), the

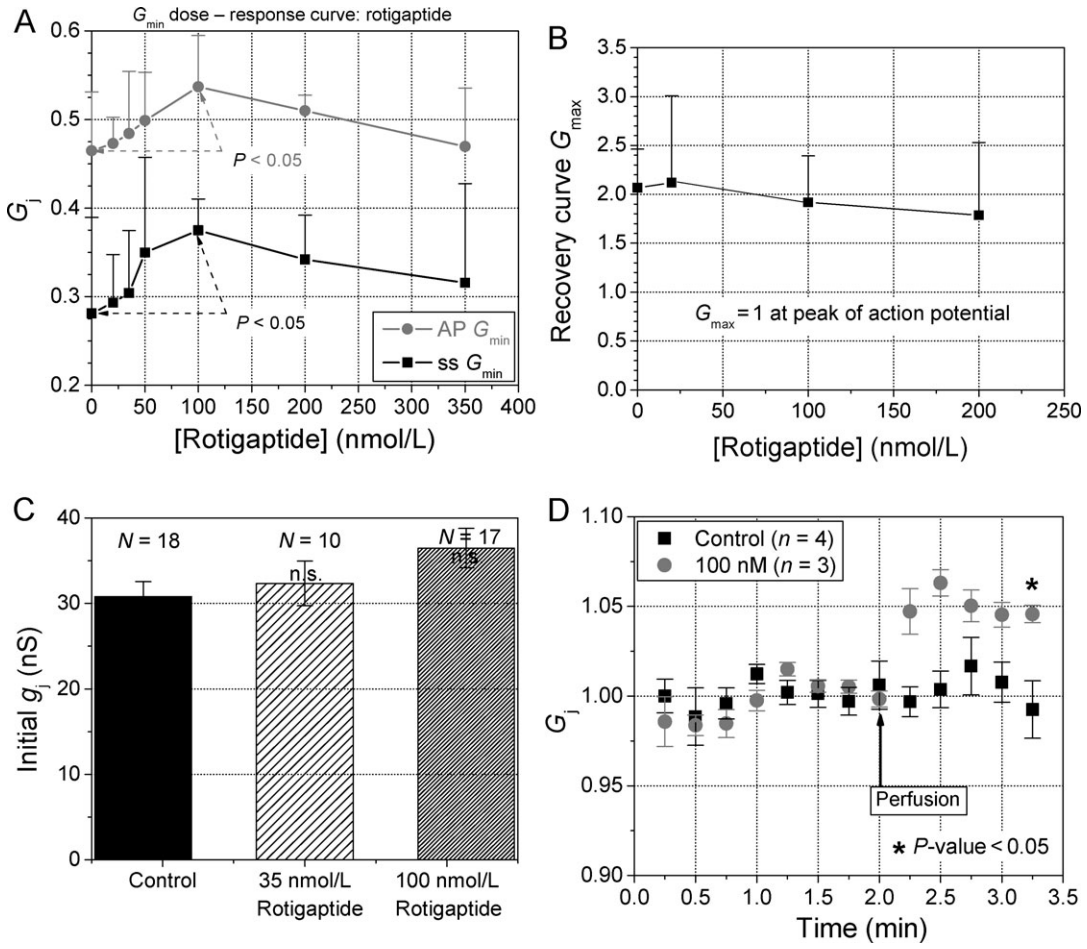

Figure 3 Rotigaptide increases the G_{min} of ventricular gap junctions. (*A*) The V_j-insensitive fraction of the total ventricular normalized junctional conductance (G_{min}) was plotted relative to the rotigaptide concentration for each set of experiments using either the action potential or steady-state V_j ramp voltage clamp protocols. Similar results for both protocols demonstrate that rotigaptide effectively increases the ventricular G_{min} between concentrations of 20–100 nM levels. Data points are mean $\pm$ SD. The maximal 10% increase in G_{min} was statistically significant from control values ($P < 0.05$, $n = 7$). (*B*) Average G_{max} of the steady-state G_j–V_j recovery curves (=$G_{max,\ rec}$), plotted relative to rotigaptide concentration, illustrates the lack of dose-dependent effects on the magnitude of facilitation. (*C*) Increase in initial g_j observed with overnight treatment with the indicated concentrations of rotigaptide. Measured immediately upon establishment of the dual whole cell patch configuration, initial g_j was elevated by an average of 5% at 35 and nearly 20% at 100 nM rotigaptide, although none of these increases were statistically significant (one-way ANOVA, $P > 0.05$). (*D*) Acute exposure to 100 nM rotigaptide by rapid bath superfusion increased g_j by 4.6% compared with control saline.

value of $G_{max,\ rec}$ for the steady-state G_j–V_j curve provides the most reliable quantitative measure of the amount of facilitation present in each ventricular cell pair recording. Averaging the $G_{max,\ rec}$ values obtained with both V_j polarities, the mean ($\pm$SEM) $G_{max,\ rec}$ ranged from 1.79 $\pm$ 0.33 to 2.12 $\pm$ 0.40 for both respective control and rotigaptide treatment groups, thus indicating no statistical difference in facilitation ($P > 0.20$, $n \geq 5$, *Figure 3B*). In agreement with previous reports,[19] a trend towards increasing initial g_j values measured immediately after achieving the dual whole cell configuration, was also observed (*Figure 3C*). A 5 or 18.5% increase in initial g_j, up from 30.8 $\pm$ 1.7 nS, was observed with 35 or 100 nM rotigaptide treatments. These initial g_j measurements were limited by the whole cell electrode series resistances and, thus, underestimate the actual g_j. To further test for increases in resting g_j, 100 nM rotigaptide was perfused onto ventricular cell pairs that exhibited a stable g_j after the rundown period (*Figure 3D*). Ventricular g_j, measured during +20 mV V_j pulses, was unchanged during control bath saline perfusion compared with acute rotigaptide treatments, which significantly increased g_j, by +4.6 $\pm$ 0.1% (P-value < 0.05). The average ventricular g_j was 14.7 $\pm$ 4.2 nS ($n = 4$) and 19.5 $\pm$ 5.2 nS ($n = 3$) for the control and 100 nM rotigaptide experiments, respectively. No changes in single channel conductances (γ_j) were observed (data not shown).

3.2 Kinetic analysis of the effects of rotigaptide

In addition to the rotigaptide-induced increase in G_{min}, the first order inactivation kinetics of ventricular gap junctions was fully examined. The ensemble averaged I_j from 5 to 10 square V_j steps of fixed magnitude and duration were fit with a biexponential decaying function to determine the fast and slow decay time constants (τ_{fast} and τ_{slow}) for each V_j. The closing on-rates for the fast and slow inactivation gating mechanisms were then calculated from the respective τ_{decay} and P_o values (see **Methods**). The ventricular gap junction fast and slow inactivation kinetics is summarized for control, 35, or 100 nM rotigaptide treatment groups in *Figure 4*. The fast and slow inactivation components were similarly affected by rotigaptide treatment and were well described by an exponentially increasing function with similarly constant V_j-dependencies of 21.0 $\pm$

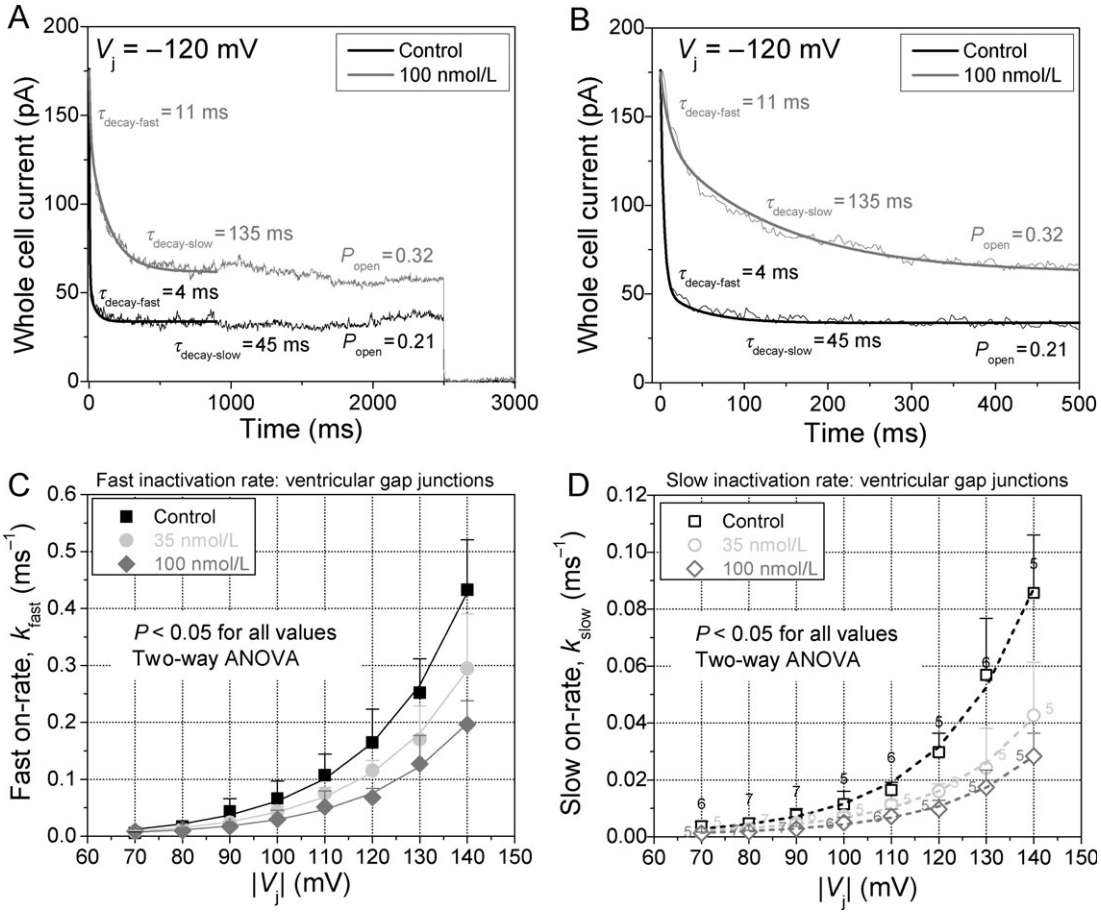

Figure 4 Effects of rotigaptide on fast and slow ventricular G_j inactivation kinetics. (*A*) Biexponential fit of the decay in whole cell 2 current to obtain the fast and slow decay time constants in response to a −120 V_j step. The fast and slow inactivation on-rates were calculated under control and 100 nM rotigaptide treatments for these ventricular myocyte cell pairs of similar g_j. (*B*) The same current traces in (A) plotted on an expanded time scale to better illustrate the exponential fit of the fast inactivation component. (*C*) The V_j-dependent fast inactivation rates of ventricular G_j inactivation was progressively slowed by increasing doses of rotigaptide. (*D*) The slow inactivation component was similarly affected by rotigaptide treatment. The number above each symbol indicates the number of experiments for the data in (C) and (D). The parameters for the fitted curves are provided in Supplementary material online, *Table S2*.

0.2 and 19.7 ± 0.3 mV, respectivly (see Supplementary material online, *Table S2*). The average V_j constant for both inactivation components was 20.3 ± 0.7 mV, identical to the previously reported value obtained from monoexponential fits of I_j τ_{decay}.[12] These data are the first description of the V_j-dependence of the macroscopic fast and slow inactivation gating mechanisms for ventricular gap junctions, which are in agreement with our previous report of the V_j-sensitivity of the slow inactivation rates.[12] The V_j-dependence is similar for the fast and slow inactivation components and is not altered by rotigaptide treatment. Two-way ANOVA analysis of the fast and slow on-rates for each V_j examined indicated a statistically significant ($P < 0.05$) slowing of both inactivation rates for $V_j > 70$ mV when comparing the control, 35 nM, and 100 nM rotigaptide treatment groups ($P < 0.05$). The V_j-dependent changes in both inactivation rates were statistically significant when $V_j > 100$ mV. The concentration-dependent effects of rotigaptide on the fast and slow inactivation rates were well described by the monoexponential functions (ms^{-1}):

$$A_{fast} = 0.01085 \cdot \exp[-[\text{rotigaptide}]/(57.7\,\text{nM})] + 0.00484 \quad (4)$$

and

$$A_{slow} = 0.00168 \cdot \exp[-[\text{rotigaptide}]/(30.0\,\text{nM})] + 0.00072 \quad (5)$$

between the concentrations of 0–100 nM.

3.3 Modelling the actions of rotigaptide on ventricular gap junctions

In order to develop a realistic mathematical model for the action of rotigaptide on the gating kinetics of ventricular gap junctions, the G_j- time curves for the BCL = 1000 ms action potential were fit with the equations for the previously published dynamic ventricular gap-junction model.[12] In *Figure 5*, the average time-dependent G_j curves for 0, 35, 100, and 350 nM rotigaptide illustrated in *Figure 1* were fit with a series of expressions developed to accurately describe the two observed inactivation and recovery components of ventricular G_j (see Supplementary material, online). *Figure 5* results demonstrate that accurate time- and V_j-dependent descriptions of the 1/s action potential G_j curve can be achieved using this model based primarily on the inactivation kinetics described in Eqs. (4)

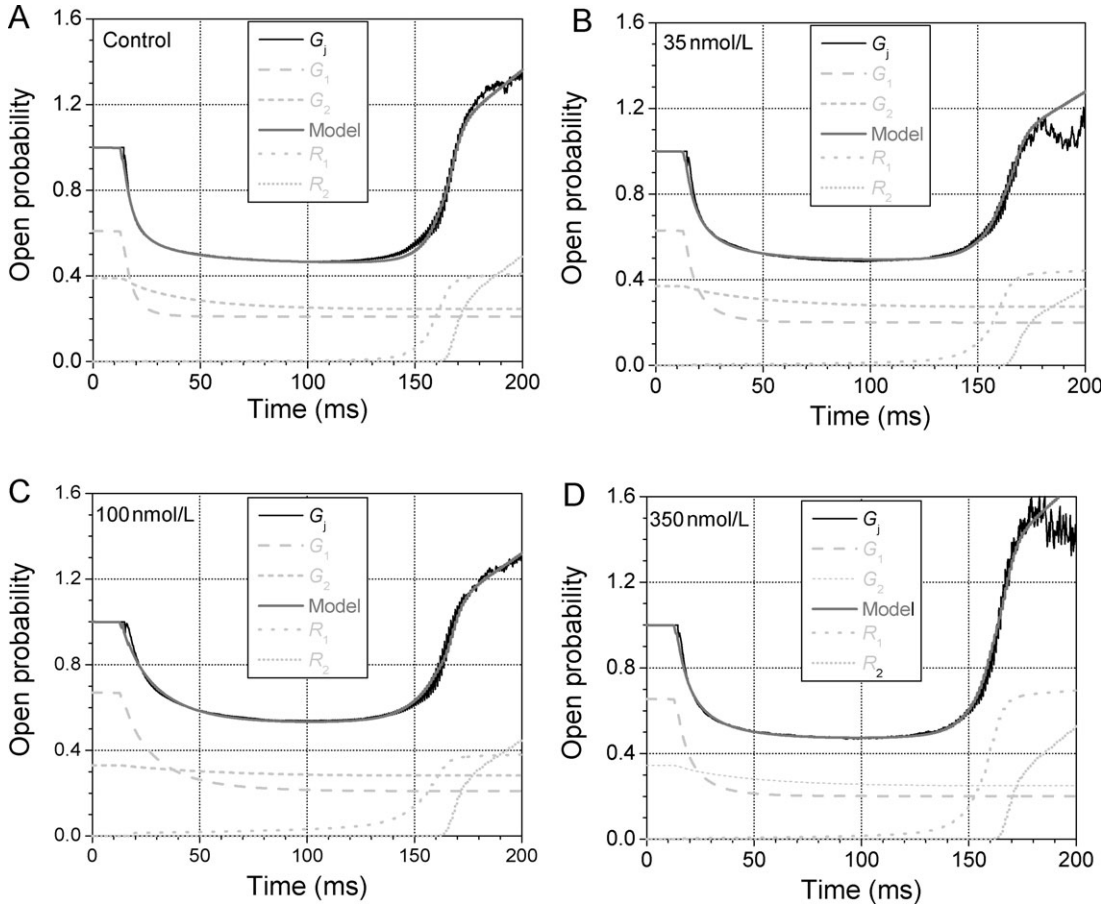

Figure 5 Dynamic ventricular gap-junction model description of rotigaptide action. The output of the current dynamic ventricular gap-junction model (grey line) accurately fitted to the control G_j (*A*), the 35 nM rotigaptide G_j (*B*), 100 nM rotigaptide G_j (*C*), and the 350 nM rotigaptide G_j (*D*) curves. The model fits were obtained by changing the amplitude of the fast and slow inactivation kinetics (G_1 and G_2, light grey dashed and short dashed lines) with only minor adjustments to the threshold voltage for the initiation of the early recovery process (R_1, light grey dotted line). The experimental G_j value was set equal to 1 when V_j = 0 and the summed output of the model was defined to be equal to this peak G_j during the diastolic period. See Supplementary material, online, for additional details.

and (5). The rotigaptide concentration-dependent values of A_1 and A_2 were determined from the above-given expressions for A_{fast} and A_{slow} with the exceptions of the 200 and 350 nM values which were determined by fitting the G_j–time curves by eye (see Supplementary material, online). These data demonstrate that the effects of rotigaptide on the gating of cardiac gap junctions can be adequately modelled by the concentration-dependent changes in the inactivation kinetics plus a slight concentration-dependent shift in the early recovery phase of ventricular G_j towards higher declining V_j values. All other model-dependent parameters remained essentially constant and independent of [rotigaptide].

3.4 Modelling ventricular action potential propagation

A major premise of this study was to determine the mechanisms by which rotigaptide preserves conduction velocity (θ) during episodes of metabolic inhibition.[8] One hypothesis is that during slow, discontinuous propagation at low levels of coupling (low g_j), V_j-dependent inactivation produces further reductions in θ than a static decrease in g_j alone. To model this behaviour, the dynamic ventricular gap-junction equations for fast and slow inactivation were programmed into a linear cable model of a cardiac strand (see Supplementary material, online).[12] Each 11 μm diameter, 100 μm long model segment (cell) was programmed with the updated Luo–Rudy II ventricular action potential and all 100 segments were uniformly coupled by a resting (initial) g_j value.[20] The resting g_j value was either kept constant (static), or allowed to inactivate during action potential propagation according to the fast and slow inactivation kinetics described in the original dynamic ventricular gap-junction model (2005 model) or in the control experiments defined herein in the absence of rotigaptide (dynamic) (see Supplementary material, online). To simulate the effects of rotigaptide, the 0–100 nM concentration-dependent reductions in the fast and slow inactivation rates were calculated according to Eqs. (4) and (5).

The calculated θ for the stable propagating action potential agrees closely with previous simulations using a constant reduction in g_j to model the effects on conduction.[21] The basis for the 20% higher maximum θ of 64 cm/s is that the newest version of the Luo–Rudy II[20] model has a higher maximum upstroke velocity (V_{max}) than the original version.[16] At first glance, it appears that the relationship between θ and g_j is not affected by the introduction of V_j-dependent gating (*Figure 6A*). However, it was postulated that inactivation would only affect g_j below 10 cm/s since

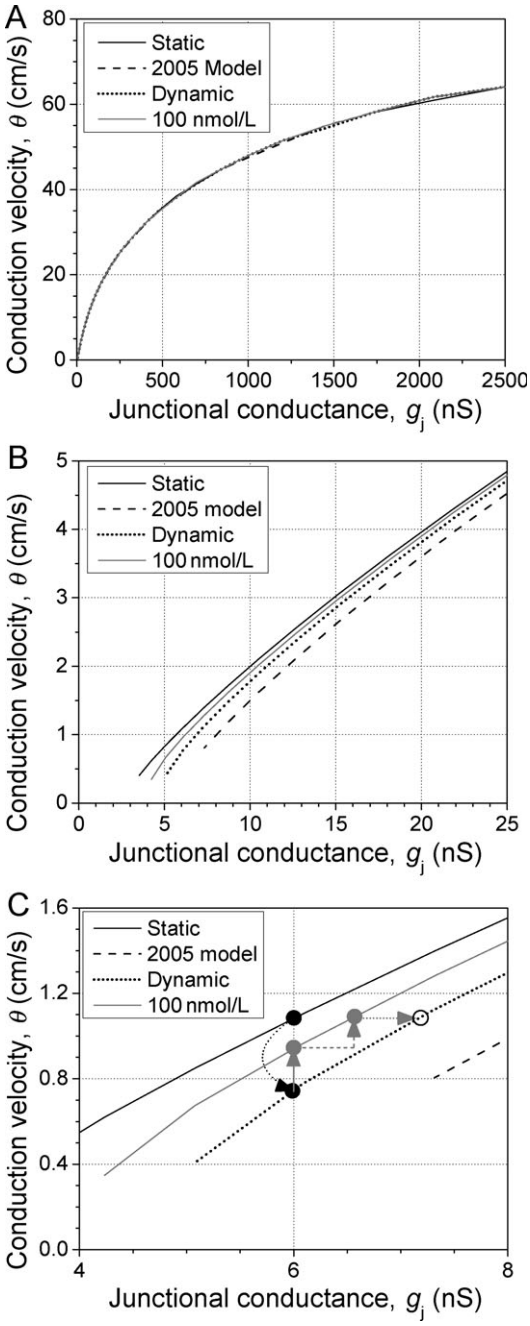

Figure 6 Effect of changing g_j on action potential conduction velocity (θ). (*A*) Ventricular θ slows from a maximum of 64 to <1 cm/s as g_j is reduced from 2500 to <5 nS. At high g_j values, no variations in θ are observed as a result of V_j-dependent gap-junction inactivation. (*B*) Discrepancies in θ are apparent at low resting g_j values, depending on the gap-junction inactivation rates that are utilized, and block develops at higher values than if g_j is kept constant during action potential propagation. (*C*) The optimal dose of 100 nM rotigaptide can completely prevent the conduction slowing produced by V_j-dependent g_j gating (black dotted arrow) via a reduction in the inactivation kinetics (solid grey arrow) coupled with a 10% increase in resting g_j (dashed grey arrow). A 20% increase in resting g_j is also sufficient to reverse the conduction slowing without alteration of the g_j inactivation kinetics (dotted grey arrow).

this is the value of θ required to impose the entire action potential upstroke across a single cardiac gap junction.[12] At these lower g_j values, disparities are observed in θ between the various models (*Figure 6B*). The basis for the higher θ value in the control-gating model is that the fast inactivation rates were experimentally determined in the present study whereas they were extrapolated from the slow inactivation rate constants in the previous dynamic gap-junction model. Compared with the static g_j model, inactivation reduces θ by nearly a third at 6 nS of g_j (*Figure 6C*). The optimal therapeutic dose of 100 nM rotigaptide would require an increase in g_j of 10% from the resting level, in addition to the slowing of inactivation, to completely reverse the effects of inactivation on θ. A 20% increase in resting g_j, as observed experimentally, would increase θ by 14% according to this most recent dynamic g_j gating model and by 23% in the case of a static g_j. Thus, the combination of a reduction in the rate of inactivation and an increase in resting g_j of 10–20% is sufficient to reverse the effects of dynamic changes in g_j and reduced levels of electrical coupling on myocardial θ.

4. Discussion

Myocardial gap junctions formed by Cx43 and Cx40 play an important role in the establishment and modulation of arrhythmias, and their functional expression and distribution are altered by infarction, heart failure, and chronic arrythmias.[14,15,22,23] During ischaemia, intracellular resistance can triple in value and longitudinal conduction velocity can slow by 2.5-fold within 20 min.[24,25] These effects are thought to occur as a result of myocardial uncoupling secondary to intracellular Na^+ and Ca^{2+} accumulation, and may affect transverse θ more than longitudinal θ due to the relative paucity of gap junctions in the transverse direction.[26–30] In a recent study, 50 nM rotigaptide increased myocardial θ by 20% in rapidly paced guinea pig ventricles and pretreatment totally prevented the ischaemia-induced 20% increase in θ and suppressed the development of arrhythmogenic discordant T-wave alternans.[31] Yet there is almost no pharmacological therapy for these alterations in the treatment of cardiac arrhythmias. Rotigaptide and a newly synthesized Cx43 CT domain RXP-E binding peptide are the only known compounds thought to directly act on cardiac gap junctions to preserve their function.[6,32,33] Rotigaptide reportedly inhibits the rundown of myocardial conduction velocity and the occurrence of spontaneous re-entrant tachycardias during acute episodes of metabolic stress including ischaemia/reperfusion by improving cardiac g_j.[4,8,34] Rotigaptide exposure also reduces chronic infarct size and the vulnerability to acute atrial fibrillation (AF).[9,10,34] However, chronic dilated or heart failure models of AF and ventricular tachycardias of focal origin were not affected by rotigaptide administration.[34–37] In the present study, we assessed the effect of therapeutic doses of rotigaptide on the conductance and V_j-dependent kinetics of cardiac gap junctions.

Increasing concentrations of rotigaptide produced a dose-dependent increase in I_j during the 4/s, 2/s, and 1/s ventricular action potential for concentrations $\leq$100 nM (*Figure 1*). These same rotigaptide concentrations increased the non-inactivating G_{min} portion of the steady-state ventricular G_j–V_j relationships, but had no effect on the increased G_j observed during the recovery phase of the steady-state G_j–V_j curves (*Figures 2* and *3*). A trend towards higher resting g_j values was also observed in ventricular cell pairs treated overnight with 35 or 100 nM rotigaptide

compared with untreated controls, although the results did not achieve statistical significance (*Figure 3C*). The rotigaptide-induced increase in ventricular g_j was confirmed by acute exposure to 100 nM concentrations by bath superfusion (*Figure 3D*). The relative increase in I_j during the action potential could be explained by the concentration-dependent effects of rotigaptide on the fast and slow inactivation rates of ventricular g_j (*Figure 4*). Further kinetic analysis revealed that both inactivation processes possess nearly identical V_j-dependencies that were unaltered by rotigaptide (see Supplementary material, online). We had previously characterized the V_j-dependence of only the slow inactivation rate of ventricular gap junctions, which increased e-fold for every 20.3 mV increase in V_j.[12] The values obtained in this study in the presence or absence of rotigaptide were essentially the same, changing e-fold for every 21.0 ± 0.2 mV or 19.7 ± 0.3 mV, respectively, for the fast or slow inactivation rates. This V_j-dependence results in significant increases in both gap-junction inactivation rates when $V_j > 100$ mV, consistent with our previous findings, and were significantly altered by 35 or 100 nM rotigaptide.[12,38] Despite the shorter APDs of higher frequencies of stimulation, ischaemia, or intrinsic ionic currents, reductions in g_j can occur as a result of inactivation and, therefore, be antagonized by rotigaptide treatment (*Figure 1E* and *F* and Supplementary material online, *Figure S4*).[18]

These results were sufficient to provide a mathematical basis for calculating the effects of rotigaptide on ventricular G_j inactivation during the normal action potential. From a functional perspective, the inactivation process corresponds to the on-rates for the fast and slow inactivation gates that close the ventricular gap-junction channels in response to large V_j gradients. The recovery phase of G_j corresponds to the reopening of these channels from inactivation, which apparently occurs by a different protein conformational shift since hysteresis was evident between the inactivation and recovery G_j–V_j curves (*Figure 2*).[12] The original dynamic ventricular gap-junction model,[12] consisting of two inactivation and recovery components for G_j, was utilized to fit the G_j-time plots for the various test concentrations of rotigaptide. It was determined that the concentration-dependent effects of rotigaptide on the gating of ventricular gap junctions could be accurately described by alterations in the fast and slow inactivation kinetics and an increase in the V_j-sensitivity of the early (R_1) recovery process. It should be noted that these predictions are based on the inactivation kinetics at 20°C, not normal body temperature. We expect the effects of g_j inactivation at 37°C to be greater than those observed in these experiments and simulations since protein conformational processes typically exhibit a Q_{10} of >2 as opposed to a diffusional process, which typically has a Q_{10} of <1.5. The temperature-dependence of cardiac gap-junction inactivation kinetics are currently being examined.

Rotigaptide, like AAP10, is thought to increase cardiac g_j by PKC activation.[39] The present results indicate that another mechanism by which rotigaptide can preserve myocardial g_j is by altering the gap-junction inactivation kinetics. There was no obvious effect of 0–100 nM rotigaptide treatments on ventricular gap-junction formation in cardiomyocyte cultures (see Supplementary material, online). Whether or not PKC stimulation and inhibition can explain the action of rotigaptide on the gating kinetics of cardiac gap junctions is currently being investigated. An additional explanation is that alternative phosphorylation sites also participate in ischaemia-induced uncoupling and that rotigaptide delays the dephosphorylation of the PKC-dependent S368 and other previously unidentified sites on Cx43.[40]

One prediction of the dynamic ventricular gap-junction model is that the gating induced by finite intercellular conduction delays will produce further slowing of myocardial conduction velocity, thus promoting slow, discontinuous propagation at higher resting g_j values than that previously modelled using static g_j values (*Figure 6*).[21] The slow θ that can be achieved only by reductions in g_j can promote the formation of unidirectional conduction block and re-entrant arrhythmias within the inhomogeneous myocardium.[14,41,42] Our present results using the updated dynamic ventricular gap-junction model, and a previous computer simulation study of a dynamic junctional resistance, both indicate that V_j-dependent inactivation will enhance these low g_j conduction delays and produce conduction block at higher initial g_j values than would occur without gating.[12,43] The major question being asked by this study is whether the observed changes in myocardial g_j are sufficient to account for the preservation of θ observed in ischaemic or diseased cardiac tissues or whole heart preparations by rotigaptide administration.[8,33,35,36] Our computer simulations, using the gap-junction inactivation kinetics described in this study, reveal that V_j-dependent gating of ventricular gap junctions will gradually slow action potential propagation at velocities below 10 cm/s. More importantly, the effect of therapeutic doses of rotigaptide on the inactivation kinetics is sufficient to prevent 60% of this conduction slowing (*Figure 6C*). Combined with a slight increase in g_j of 10%, rotigaptide can effectively abolish the conduction slowing observed under partially uncoupled conditions. Our computer simulations also indicate that the same improvement in myocardial θ can be achieved by a 20% increase in resting g_j, consistent with an experimentally observed trend that did not quite achieve statistical significance ($P = 0.07$ at 100 nM rotigaptide, $N = 17$). This preservation of myocardial g_j by rotigaptide may be sufficient, under certain circumstances, to prevent the formation of unidirectional block or lengthen the required re-entrant pathway beyond a sustainable limit needed for the formation of re-entrant tachycardias. This latter hypothesis will require further investigation. In conclusion, experimental evidence and computer simulations demonstrating the dynamic alterations of the gating of ventricular gap junctions provides further insight into the mechanisms by which rotigaptide can preserve myocardial conduction during acute ischaemic episodes. Additional experiments are required to determine the molecular bases for the kinetic modulation of cardiac gap junctions by rotigaptide and the mechanisms responsible for myocardial uncoupling and conduction slowing during episodes of metabolic stress.

Supplementary material

Supplementary material is available at *Cardiovascular Research* online.

Acknowledgements

We would like to acknowledge the contribution of the 1 Hz neonatal murine ventricular action potential waveform by Ms Linda J. Wang, Harvard Medical School, Boston, MA, USA and Dr Eric A. Sobie, Mount Sinai School of Medicine, New York, NY, USA.

Conflict of interest: this work was performed with rotigaptide provided by permission from Wyeth Research and licensed for use in US by Wyeth from Zealand Pharma A/S, Glostrup, Denmark. R.D.V. is a paid consultant of Wyeth Research. J.K.H. is an employee of Wyeth Research. J.S.P. is the Chief Scientific Officer and Vice President of Zealand Pharma A/S.

Funding

National Institutes of Health, National Heart, Lung and Blood Institute grant HL-042220 (R.D.V.) and Wyeth Research, Cardiovascular and Metabolic Diseases Division, Collegeville, PA, USA (R.D.V.).

References

1. Poelzing S, Akar FG, Baron E, Rosenbaum DS. Heterogeneous connexin43 expression produces electrophysiological heterogeneities across ventricular wall. *Am J Physiol Heart Circ Physiol* 2004;**286**: H2001–H2009.
2. Gutstein DE, Morley GE, Vaidya D, Liu F, Chen FL, Stuhlmann H *et al*. Heterologous expression of gap junction channels in the heart leads to conduction defects and ventricular dysfunction. *Circulation* 2001;**104**: 1194–1199.
3. Gutstein DE, Danik SB, Lewitton S, France D, Liu F, Chen FL *et al*. Focal gap junction uncoupling and spontaneous ventricular ectopy. *Am J Physiol Heart Circ Physiol* 2005;**289**:H1091–H1098.
4. Xing D, Kjølbye AL, Nielsen MS, Petersen JS, Harlow KW, Holstein-Rathlou NH *et al*. ZP123 increases gap junctional conductance and prevents reentrant ventricular tachycardia during myocardial ischemia in open chest dogs. *J Cardiovasc Electrophysiol* 2003;**14**: 510–520.
5. Herve JC, Dhein S. Pharmacology of cardiovascular gap junctions. *Adv Cardiol* 2006;**42**:107–131.
6. Nattel S, Carlsson L. Innovative approaches to anti-arrhythmic drug therapy. *Nat Rev Drug Disc* 2006;**5**:1034–1049.
7. Clark TC, Thomas D, Petersen JS, Evans WH, Martin PEM. The anti-arrhythmic pewptide rotigaptide (ZP123) increases gap junction intercellular communication in cardiac myocytes and HeLa cells expressing connexin43. *Brit J Pharmacol* 2006;**147**:486–495.
8. Haugan K, Olsen KB, Hartvig L, Petersen JS, Holstein-Rathlou NH, Hennan JK *et al*. The antiarrhythmic peptide analog ZP123 prevents atrial conduction slowing during metabolic stress. *J Cardiovasc Electrophysiol* 2005;**16**:537–545.
9. Haugan K, Marcussen N, Kjølbye AL, Nielsen MS, Hennan JK, Petersen JS. Treatment with the gap junction modifier rotigaptide (ZP123) reduces infarct size in rats with chronic myocardial infarction. *J Cardiovasc Pharmacol* 2006;**47**:236–242.
10. Hennan JK, Swillo RE, Morgan GA, Keith JC Jr, Schaub RG, Smith RP *et al*. Rotigaptide (ZP123) prevents spontaneous ventricular arrhythmias reduces infarct size during myocardial ischemia/reperfusion injury in open-chest dogs. *J Pharmacol Exp Ther* 2006;**317**:236–243.
11. Kjølbye AL, Haugan L, Hennan JK, Petersen JS. Pharmacological modulation of gap junction function with the novel compound Rotigaptide: a promising new principle for prevention of arrhythmias. *Basic Clin Pharmacol Toxicol* 2007;**101**:215–230.
12. Lin X, Gemel J, Beyer EC, Veenstra RD. Dynamic model for ventricular junctional conductance during the cardiac action potential. *Am J Physiol Heart Circ Physiol* 2005;**288**:H1113–H1123.
13. Weingart R, Maurer P. Action potential transfer in cell pairs isolate from adult rat and guinea pig ventricles. *Circ Res* 1988;**63**:72–80.
14. Kléber AG, Rudy Y. Basic mechanisms of cardiac impulse propagation and associated arrhythmias. *Physiol Rev* 2004;**84**:431–488.
15. Nattel S, Maguy A, Le Bouter S, Yeh T-S. Arrhythmogenic ion-channel remodeling in the heart: heart failure, myocardial infarction, and atrial fibrillation. *Physiol Rev* 2007;**87**:425–456.
16. Veenstra RD. Voltage clamp limitations of dual whole-cell gap junction current and voltage recordings. I. Conductance measurements. *Biophys J* 2001;**80**:2231–2247.
17. Luo C-H, Rudy Y. A dynamic model of the cardiac ventricular action potential. I. Simulations of ionic currents and concentration changes. *Circ Res* 1994;**74**:1071–1096.
18. Wang LJ, Sobie EA. Mathematical model of the neonatal mouse action potential. *Am J Physiol Heart Circ Physiol* 2008; Epub ahead of print 11 April 2008.
19. Dhein S. Pharmacology of gap junctions in the cardiovascular system. *Cardiovasc Res* 2004;**62**:287–298.
20. Faber GM, Rudy Y. Action potential and contractility changes in. Action potential and contractility changes in [Na(+)](i) overloaded cardiac myocytes: a simulation study. *Biophys J* 2000;**78**:2392–2404.
21. Shaw RM, Rudy Y. Ionic mechanisms of propagation in cardiac tissue. Roles of the sodium and L-type calcium currents during reduced excitability and decreased gap junction coupling. *Circ Res* 1997;**81**: 727–741.
22. Luke RA, Saffitz JE. Remodeling of ventricular conduction pathways in healed canine infarct border zones. *J Clin Invest* 1991;**87**: 11594–11602.
23. Cabo C, Yao J, Boyden PA, Chen S, Hussain W, Duffy HS *et al*. Heterogeneous gap junction remodeling in reentrant circuits in the epicardial border zone of the healing canine infarct. *Cardiovasc Res* 2006;**72**: 241–249.
24. Kléber AG, Riegger CB, Janse MJ. Electrical uncoupling and increase of extracellular resistance after induction of ischemia in isolated, arterially perfused rabbit papillary muscle. *Circ Res* 1987;**61**:271–279.
25. Cascio WE, Yang H, Johnson TA, Muller-Borer BJ, Lemasters JJ. Electrical properties and conduction in reperfused papillary muscle. *Circ Res* 2001; **89**:807–814.
26. De Mello WC. Effect of intracellular injection of calcium and strontium on cell communication in the heart. *J Physiol* 1975;**250**:231–245.
27. De Mello WC. Uncoupling of heart cells produced by intracellular sodium injection. *Experentia* 1975;**31**:460–461.
28. Weingart R. The actions of ouabain on intercellular coupling and conduction velocity in mammalian ventricular muscle. *J Physiol* 1977;**264**: 341–365.
29. Spach MS, Kootsey JM, Sloan JD. Active modulation of electrical coupling between cardiac cells of the dog. A mechanism for transient and steady state variations in conduction velocity. *Circ Res* 1982;**51**: 347–362.
30. Kléber AG. Consequences of acute ischemia for the electrical and mecjhanical function of the ventricular myocardium. A brief review. *Experentia* 1990;**46**:1162–1167.
31. Kjølbye AL, Dikshteyn M, Eloff BC, Deschênes I, Rosenbaum DS. Mantenance of intercellular couopling by the antiarrhythmic peptide rotigaptide suppresses arrhythmogenic discordant alternans. *Am J Physiol Heart Circ Physiol* 2008;**294**:H41–H49.
32. Shibayama J, Lewandowski R, Kieken F, Coombs W, Shah S, Sorgen PL *et al*. Identification of a novel peptide that interferes with the chemical regulation of connexin43. *Circ Res* 2006;**98**:1365–1372.
33. Eloff BC, Gilat E, Wan X, Rosenbaum DS. Pharmacological modulation of cardiac gap junctions to enhance cardiac conduction: evidence supporting a novel target for antiarrhythmic therapy. *Circulation* 2003;**108**: 3157–3163.
34. Shiroshita-Takeshita A, Sakabe M, Haugan K, Hennan JK, Nattel S. Model-dependent effects of the gap junction conduction-enhancing antiarrhytmic peptide rotigaptide (ZP123) on experimental atrial fibrillation in dogs. *Circulation* 2007;**115**:310–318.
35. Guerra JM, Everett TH, Lee KW, Wilson E, Olgin JE. Effects of the gap junction modifier rotigaptide (ZP123) on atrial conduction and vulnerability to atrial fibrillation. *Circulation* 2006;**114**:110–118.
36. Haugen K, Miyamoto T, Takeishi Y, Kubota I, Nakayama J, Shimojo H *et al*. Rotigaptide (ZP123) improves atrial conduction slowing in chronic volume overload-induced dilated atria. *Basic Clin Pharmacol Toxicol* 2006;**99**: 71–79.
37. Xing D, Kjølbye AL, Petersen JS, Martins JB. Pharmacological stimulation of cardiac gap junction coupling does not affect ischemia-induced focal ventricular tachycardia or triggered activity in dogs. *Am J Physiol Heart Circ Physiol* 2005;**288**:H511–H516.
38. Lin X, Crye M, Veenstra RD. Regulation of connexin43 gap junctional conductance by ventricular action potentials. *Circ Res* 2003;**93**:e63–e73.

39. Weng S, Lauven M, Schaefer T, Polontchouk L, Grover R, Dhein S. Pharmacological modification of gap junction coupling by an anti-arrhythmic peptide via protein kinase C activation. *FASEB J* 2002;**16**: 1114–1116.
40. Axelsen LN, Stahlhut M, Mohammed S, Larsen BD, Nielsen MS, Holstein-Rathlou N-H *et al*. Identification of ischemia-regulated phosphorylation sites in connexin43: a possible target for the antiarrhythmic peptide analogue rotigaptide (ZP123). *J Molec Cell Cardiol* 2006;**40**: 790–798.
41. Quan W, Rudy Y. Unidirectional block and reentry of cardiac excitation: a model study. *Circ Res* 1990;**66**:367–382.
42. Joyner RW, Sugiura H, Tan RC. Unidirectional block between isolated rabbit ventricular cells coupled by a variable resistor. *Biophys J* 1991; **60**:1038–1045.
43. Henriquez AP, Vogel R, Muller-Borer BJ, Henriquez CS, Weingart R, Cascio WE. Influence of dynamic gap junction resistance on impulse propagation in ventricular myocardium: a computer simulation study. *Biophys J* 2001;**81**:2112–2121.